

Graphite Electrode Modified with a New Phenothiazine Derivative and with Carbon Nanotubes for NADH Electrocatalytic Oxidation

D. Gligor, C. Varodi, and L. M. Muresan*

“Babes-Bolyai” University, Department of Physical Chemistry,
11 Arany Janos St., 400028 Cluj-Napoca, Romania

Original scientific paper

Received: May 12, 2009

Accepted: December 18, 2009

The electrochemical behavior of a modified electrode obtained by immobilization of single-walled carbon nanotubes onto a graphite electrode modified with a new phenothiazine derivative, bis-phenothiazin-3-yl methane (BPhM), G/BPhM-CNT, has been evaluated and compared with BPhM adsorbed on graphite electrode (G/BPhM). The G/BPhM-CNT electrode presents improved performances for NADH electrocatalytic oxidation in comparison with G/BPhM electrode, expressed by: (i) a significant increase of electrocatalytic rate constant ($k_{\text{obs},[\text{NADH}] = 0}$) for NADH oxidation ($856.32 \text{ L mol}^{-1} \text{ s}^{-1}$ for G/BPhM-CNT and $51.63 \text{ L mol}^{-1} \text{ s}^{-1}$ for G/BPhM, in phosphate buffer, pH 7); (ii) the obtained amperometric sensors for NADH detection present increase sensitivity ($S = 6.9 \text{ mA L mol}^{-1}$ for G/BPhM-CNT and $S = 0.55 \text{ mA L mol}^{-1}$ for G/BPhM, pH 7).

Key words:

Phenothiazine derivative, carbon nanotubes, NADH

Introduction

Carbon nanotubes (CNTs) have attracted much attention due to their high chemical stability, high surface area, unique electronic properties, and relatively good mechanical properties. The physical and chemical properties of CNTs make them a good nano-structured material for different applications in a wide range of technological fields including chemistry, biology, medicine, electronics, materials and engineering.^{1–3} When compared with other forms of carbon electrodes such as graphite and bare glassy carbon electrodes, the modified electrodes based on CNTs show better performance, better conductivity and the ability to promote electron-transfer reactions. Due to the material structure (channels inherently exist in the tubes), the electronic structure, and the topological defects present on the tube surface, they are successfully used as electrode material in electrochemical reactions.^{4–6}

The reported electrodes based on CNTs were usually prepared by casting the CNTs solution onto the electrode surface (binder free) or by dispersing CNTs in a binder, such as *N,N*-dimethylformamide, Teflon, and Nafion, to form a CNTs electrode (with binder).^{7–9} CNTs intermingled with other nanomaterials (such as nano Au particles, nano ZrO_2 , etc.) were used to modify conventional electrodes. These materials provide a synergic effect that leads to the improvement in the response of modified electrodes.¹⁰

A wide variety of applications of electrodes based on CNTs for detection of bioorganic and inorganic compounds such as: NADH, neurotransmitters,^{11,12} proteins, nucleic acids, carbohydrates, micromolecules⁷ and biomacromolecules⁹ has already been reported.

The electrochemical detection of NADH is of considerable interest,¹³ since there are a large number of dehydrogenases that require this co-factor for their enzymatic reaction. Consequently, considerable effort has been devoted to the goal of identifying new electrode materials or mediators to allow the stable determination of NADH at low overpotentials.

CNTs modified electrodes exhibited an accelerated electron transfer of NADH along with minimization of surface fouling and decrease of overpotential. Several mediators for NADH detection have been reported in the literature, including quinones, oxometalates, ruthenium complexes,¹⁴ quinonoid redox dyes, for example indamines, phenazines, phenoxazines and phenothiazines.^{13–16} These redox mediators are very efficient as electron shuttles for NADH oxidation but are not always suitable for long-term monitoring of reactions involving NADH, because of their poor stability. Some are highly soluble; others lose sensitivity after deposition on electrodes or are too pH-dependent.^{14–16}

Phenothiazine derivatives can be successfully used as modifiers of electrode surfaces due to some of their characteristics: they are insoluble in water and can be easily adsorbed on graphite surface;

*Corresponding author: limur@chem.ubbcluj.ro

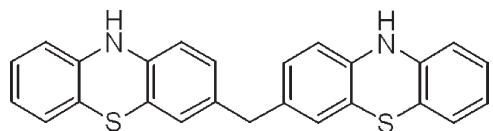
they present good kinetic parameters for heterogeneous electron transfer and for NADH electrocatalytic oxidation and can be used as redox mediators in transducers for amperometric biosensors.

In this context, the paper presents a new type of modified electrode for NADH detection obtained by immobilization of single-walled carbon nanotubes onto a graphite electrode modified with a new phenothiazine derivative (bis-phenothiazin-3-yl methane) which was proved to be a more efficient mediator for NADH oxidation than other phenothiazine derivatives.¹⁷ The electrochemical behavior of the electrode in different experimental conditions (scan rates and pH values), the electrochemical stability and the electrocatalytic behavior towards NADH oxidation were tested using cyclic voltammetry (CV) and rotating disk electrode measurements. The analytical and kinetic performances of obtained amperometric sensors for NADH detection were determined, using amperometry. The characteristics of this type of modified electrode were compared with those of a simple graphite electrode modified with the same phenothiazine derivative.

Experimental conditions

Materials

Bis-phenothiazin-3-yl methane (BPhM) was a gift from Dr. Castelia Cristea, Department of Organic Chemistry, “Babes-Bolyai” University Cluj-Napoca, (Romania). BPhM was synthesized as previously reported¹⁷ and its structure is shown in Scheme 1.



Scheme 1 – Structural formula of bis-phenothiazin-3-yl methane¹⁷

Nicotinamide adenine dinucleotide, reduced form (NADH) as disodium salt, dimethyl sulfoxide (DMSO) 99.6 % and carbon nanotubes, single-walled were purchased from Sigma (St. Louis, MO, USA) and $K_2HPO_4 \cdot 2H_2O$ and $KH_2PO_4 \cdot H_2O$ from Merck (Darmstadt, Germany). All other reagents were of analytical grade and used as received. The supporting electrolyte was a 0.1 mol L⁻¹ phosphate buffer solution.

Electrode preparation

A spectrographic graphite rod (Ringsdorff-Werke, GmbH, Bonn-Bad Godesberg, Germany), of ~ 3 mm diameter, was wet polished on fine (grit 400 and

600) emery paper (Buehler, Lake Bluff, Ill., USA). Then, a graphite piece of suitable length was carefully washed with deionized water, dried, and finally press-fitted into a PTFE holder in order to obtain a graphite electrode having, in contact with the solution, a flat circular surface area of ~ 0.071 cm².

The modified graphite electrodes (G/BPhM) were obtained by spreading onto the electrode surface 20 μ L of 5 mmol L⁻¹ phenothiazine derivative solution in dimethylsulfoxide, and leaving them for one hour at room temperature to evaporate the solvent. Before immersion in the test solution, the modified electrodes were carefully washed with deionized water. For each electrode, the surface concentration (Γ , mol cm⁻²) was estimated from the peak areas, recorded during the CV measurements at low scan rate ($v < 10$ mV s⁻¹), corrected for the background current.^{18,19}

The CNTs were immobilized onto the G/BPhM electrode by using water as the dispersing agent. The casting solution was prepared by introducing 1 mg of CNTs into 200 μ L of deionized water. A 20 μ L aliquot of this sonicated solution was placed directly onto the G/BPhM surface and left to dry, after which the electrode was ready for use.¹⁵ In this way, the G/BPhM-CNT electrode was obtained.

All presented results are the average of at least 3 identically prepared electrodes, if not otherwise mentioned.

Physical-chemical and electrochemical measurements

Microstructural characterization of the samples was performed with a scanning electronic microscope (SEM) JSM 5600 LV type (JEOL Company) equipped with EDX spectrometer (Oxford Instruments) for qualitative and quantitative microanalysis radiation X. The dried samples were measured both in the fracture and the polished surface. The fractured section was coated with a thin layer of gold.

Electrochemical experiments were carried out using a typical three-electrode electrochemical cell. The modified electrode was used as working electrode, a platinum ring as counter electrode and an Ag|AgCl/KCl_{sat} as reference electrode.

Cyclic voltammetry experiments were performed on a PC-controlled electrochemical analyzer (Autolab-PGSTAT 10, EcoChemie, Utrecht, The Netherlands).

Steady state amperometric measurements at different rotating speeds of the working electrode were performed using an EG&G rotator (Radiometer) and the same spectrographic graphite as disk material. The current–time data were collected using the above-mentioned electrochemical analyzer.

Batch amperometric measurements at different NADH concentrations were carried out at an applied potential of +100 mV vs. Ag|AgCl/KCl_{sat}, under magnetic stirring, using 0.1 mol L⁻¹ phosphate buffer solution as supporting electrolyte. The current-time data were collected using the above-mentioned electrochemical analyzer.

The pH of the phosphate buffer solutions was adjusted using NaOH or H₃PO₄ and a pH-meter (HI255, Hanna Instruments, Romania), with a combined glass electrode.

Results and discussions

Characterization of modified electrodes

Firstly, in order to check the presence of CNTs on G/BPhM-CNT surface, the G/BPhM-CNT, G/BPhM and G electrodes were characterized using SEM (Figs. 1a, 1b, and 1c, respectively). The CNTs are found to be dispersed fairly well on the surface of the G/BPhM-CNT modified electrode (Fig. 1a). The inset of Fig. 1a shows magnified image of the CNTs, the length and the typical diameter of the single-walled CNTs.

The electrochemical behavior of G/BPhM-CNT was investigated by cyclic voltammetry (Fig. 2). A clearly defined peak pair corresponding to a quasi-reversible surface immobilized redox couple, with a formal standard potential, E^0 , of -93 mV vs. Ag|AgCl/KCl_{sat} for G/BPhM-CNT, and E^0 of -56 mV vs. Ag|AgCl/KCl_{sat} for G/BPhM, respectively, was observed. The oxidation peak was attributed to the formation of stable radical cation generated by the phenothiazine structural units present in the molecular structure.²⁰ It can be observed that the G/BPhM-CNT modified electrodes exhibit a negative shift of the anodic peak potential and increased current signal towards G/BPhM, which is specific for CNTs modified electrodes.¹⁴

Cyclic voltammetric measurements were performed in a wide range of potential scan rates (from $\nu = 0.01$ to 1.28 V s⁻¹), when the electrodes were in contact with phosphate buffer solutions of different pH values (from 5 to 9). The slopes of the log-log peak current – potential scan rate dependence were close to one for both G/BPhM and G/BPhM-CNT electrodes (results not shown), indicating kinetically controlled charge transfer and confirming that the mediator is immobilized on the electrode surface.

From the dependence of the peak potentials on the potential scan rate (Fig. 3), the heterogeneous electron-transfer rate constants (k_s , s⁻¹), for the redox process corresponding to G/BPhM-CNT electrode, were estimated (Table 1) using the Laviron treatment.²¹ As can be seen, irrespective of the pH

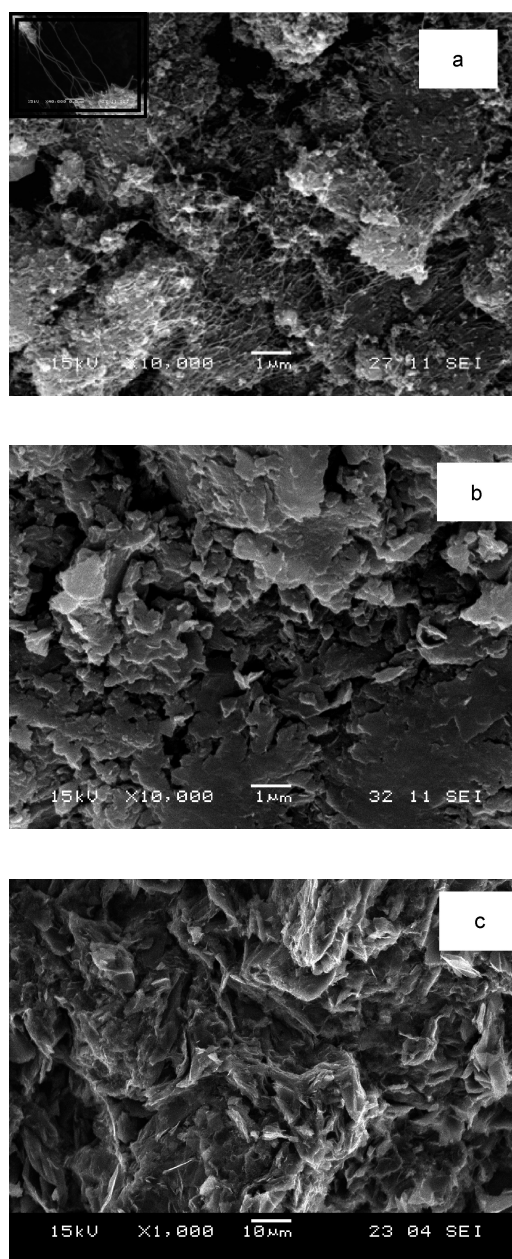


Fig. 1 – SEM micrographs of G/BPhM-CNT (a), G/BPhM (b) modified electrodes and G (c) electrodes

values, the transfer coefficients (α) are close to 0.5–0.6 and the k_s values are ~ 1.3 – 1.4 s⁻¹ for G/BPhM-CNT electrode, suggesting that the reaction pathway and the charge transfer rate remain unchanged in the investigated pH range. Also, there are no significant differences for α and k_s values, corresponding to G/BPhM and G/BPhM-CNT electrodes. However, the k_s value for G/BPhM is higher than those prepared in same way, but using smaller quantities of phenothiazine solution (0.7 s⁻¹).¹⁷

As expected for *N*-unsubstituted phenothiazine derivatives²² (Fig. 4), the standard formal potential (E^0 , estimated as the average of the cathodic and the anodic peak potentials from the cyclic

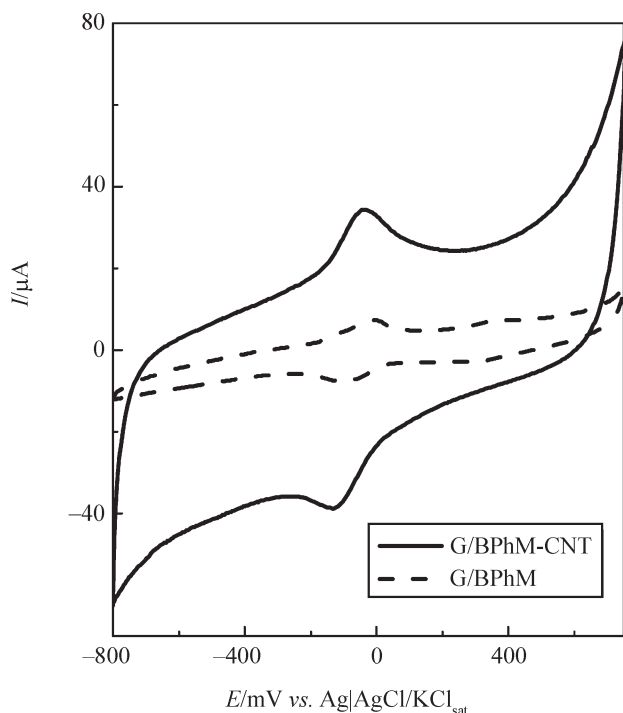


Fig. 2 – Cyclic voltammograms for G/BPhM-CNT (—) and G/BPhM (---) modified electrodes. Experimental conditions: starting potential, -800 mV vs. $\text{Ag}|\text{AgCl}/\text{KCl}_{\text{sat}}$; scan rate, 5 mV s^{-1} ; supporting electrolyte, 0.1 mol L^{-1} phosphate buffer, pH 7.

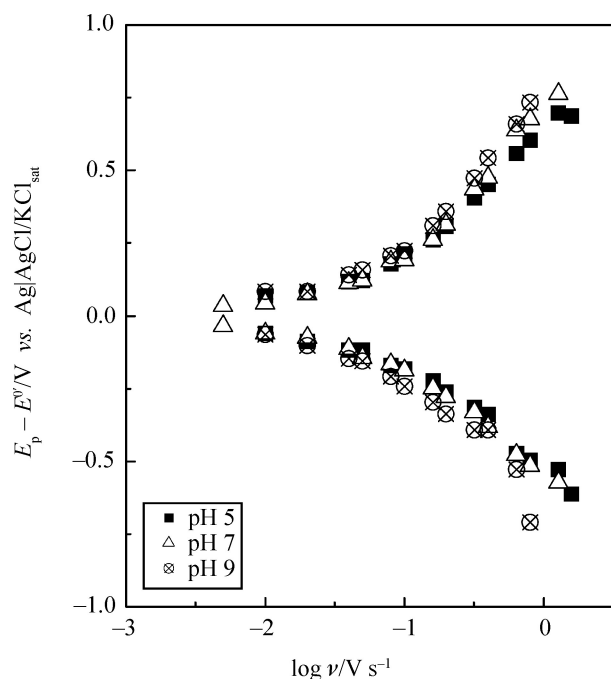


Fig. 3 – Dependence of $(E_p - E^0)$ on the logarithm of the scan rate for a G/BPhM-CNT electrode. Experimental conditions: starting potential, -800 mV vs. $\text{Ag}|\text{AgCl}/\text{KCl}_{\text{sat}}$; supporting electrolyte, 0.1 mol L^{-1} phosphate buffer.

voltammograms recorded in the pH range from 1 to 9) changes with pH ($61 \text{ mV}/\Delta\text{pH}$), as predicted for a redox process involving an equal number of protons and electrons, within experimental errors.

Table 1 – Kinetic parameters for the heterogeneous electron-transfer at G/BPhM-CNT modified electrode. Experimental conditions: as in Fig. 3.

Electrode	pH	α	k_s/s^{-1}	R/no. of exp. points		$\Gamma/\text{mol cm}^{-2}$
G/BPhM	7	0.64	1.50	0.996/7	0.994/9	$1.28 \cdot 10^{-8}$
	5	0.53	1.31	0.997/8	0.984/9	$2.98 \cdot 10^{-8}$
G/BPhM-CNT	7	0.62	1.46	0.993/7	0.991/8	$3.00 \cdot 10^{-8}$
	9	0.59	1.41	0.996/7	0.993/5	$1.81 \cdot 10^{-8}$

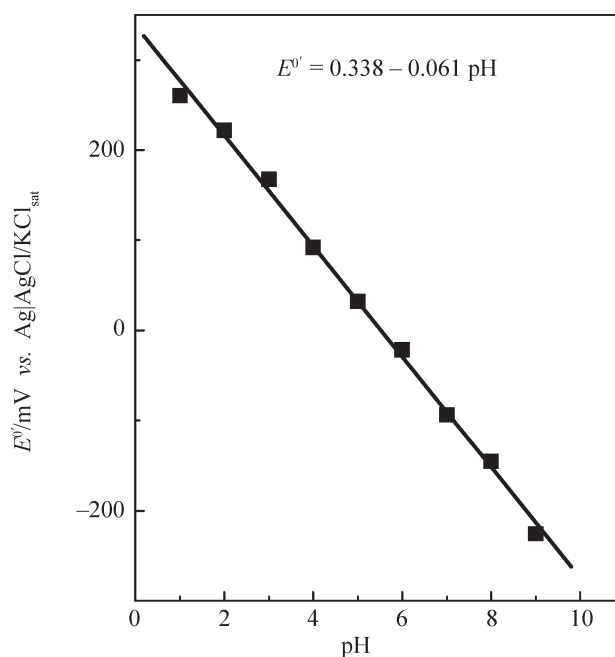


Fig. 4 – Variation of E^0 with pH for G/BPhM-CNT. Experimental conditions: starting potential, -800 mV vs. $\text{Ag}|\text{AgCl}/\text{KCl}_{\text{sat}}$; potential scan rate, 50 mV s^{-1} ; supporting electrolyte, 0.1 mol L^{-1} phosphate buffer.

The electrochemical stability of G/BPhM and G/BPhM-CNT was studied by performing repetitive measurements of cyclic voltammetry, in phosphate buffer solutions of pH 5, 7 and 9, at potential scan rate of $\nu = 50 \text{ mV s}^{-1}$. As can be observed from Fig. 5, both electrodes present a good stability, proved by small variation of surface concentration during 25 cycles, while the shape of the voltammograms remained invariant (results not shown).

NADH oxidation at G/BPhM and G/BPhM-CNT electrodes

The cyclic voltammograms recorded in phosphate buffer (pH 7) at G/BPhM and G/BPhM-CNT electrodes, in absence and in presence of different concentrations of NADH (Figs. 6a and b), revealed a good electrocatalytic activity for NADH oxidation. It can be observed the beneficial influence of CNTs on

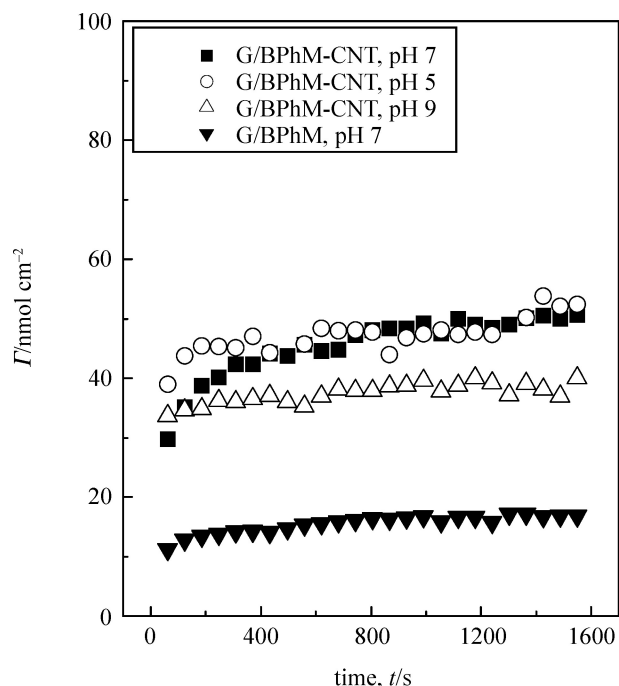


Fig. 5 – Dependence of surface concentration on cycling time for G/BPhM-CNT and G/BPhM. Experimental conditions: starting potential, -800 mV vs. Ag|AgCl/KCl_{sat}; potential scan rate, 50 mV s⁻¹; supporting electrolyte, 0.1 mol L⁻¹ phosphate buffer.

electrocatalytic oxidation of NADH, reflected in an increase of the catalytic current and decrease of the oxidation potentials, in comparison with the G/BPhM electrode. The effect was attributed to the presence of edge plane graphite sites within the walls and at the ends of carbon nanotubes.¹⁵

The electrocatalytic efficiency, estimated as the $\frac{(I_{\text{peak}})_{[\text{NADH}] = 2 \text{ mmol L}^{-1}} - (I_{\text{peak}})_{[\text{NADH}] = 0}}{(I_{\text{peak}})_{[\text{NADH}] = 0}}$ ratio, at an

applied potential of $+100$ mV vs. Ag|AgCl/KCl_{sat}, was 117 % for G/BPhM-CNT and 77 % for G/BPhM. These values are higher in comparison with those recorded for graphite electrodes modified with other phenothiazine derivatives (e.g. 3,7-di(*m*-aminophenyl)-10-ethyl-phenothiazine).²³

In order to determine the optimal applied potential, measurements of catalytic current at different applied potentials were performed by using amperometry. As can be observed from Fig. 7, the optimal value of applied potential was $+100$ mV vs. Ag|AgCl/KCl_{sat} and this value was used for all further measurements. This value of applied potential is well placed in comparison with other values used for NADH detection based on modified electrodes with carbon nanotubes, reported in the literature ($-100 \div 630$ mV).^{2,14,24–32} The marked decrease in the overvoltage for the NADH oxidation can facilitate convenient low potential stable detection of different analytes using NAD⁺-dependent dehydrogenase biosensors.

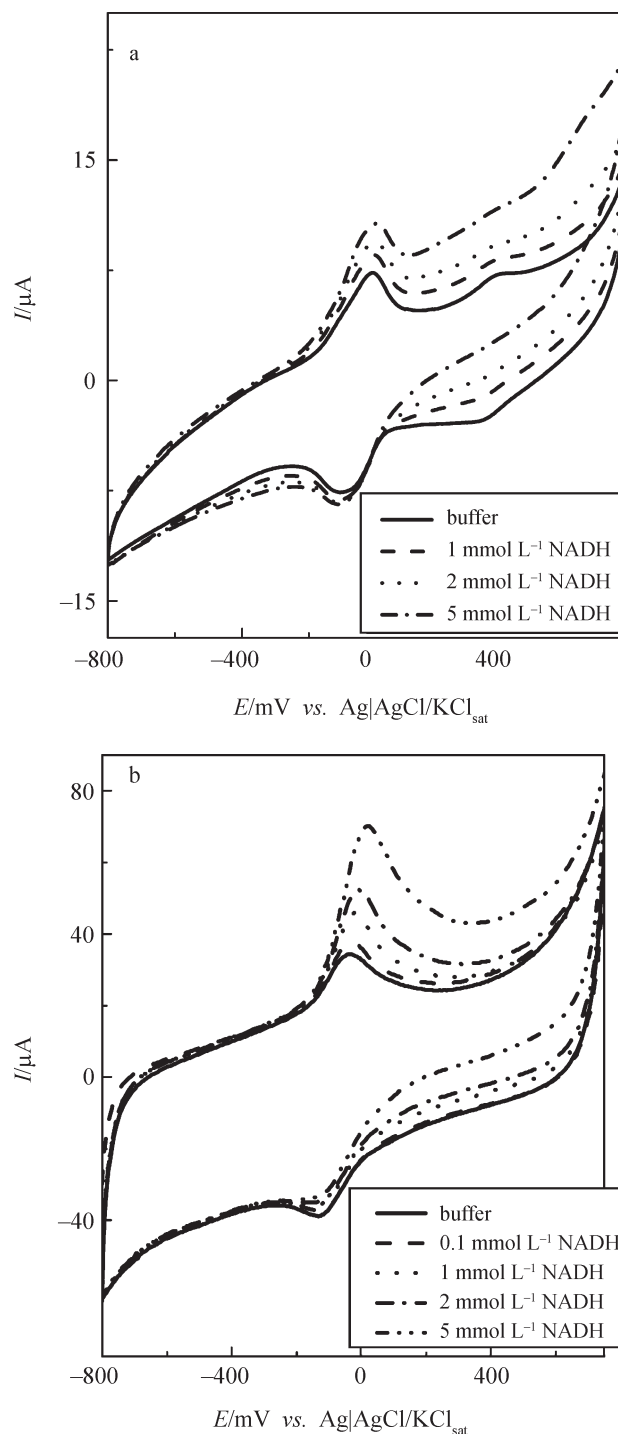


Fig. 6 – Electrocatalytic activity of (a) G/BPhM and (b) G/BPhM-CNT electrodes for NADH oxidation, in absence and in presence of different NADH concentrations. Experimental conditions: starting potential, -800 mV vs. Ag|AgCl/KCl_{sat}; scan rate, 5 mV s⁻¹; supporting electrolyte, 0.1 mol L⁻¹ phosphate buffer (pH 7.0).

In order to confirm the effect of CNTs on the reaction kinetics between NADH and phenothiazine derivative, the electrocatalytic rate constant was estimated, using rotating disk electrode experiments, at different rotation speeds and NADH concentrations.¹³ From Koutecky-Levich plot of I^{-1} vs. $\omega^{-1/2}$

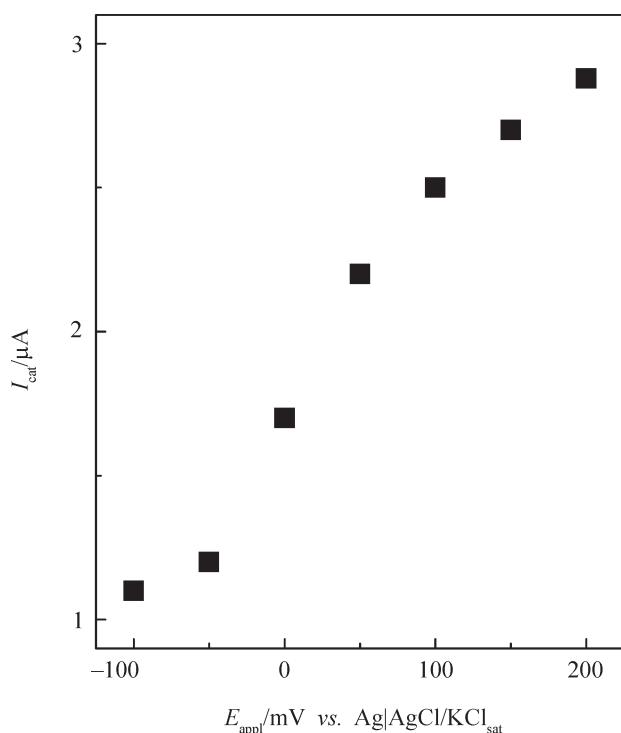


Fig. 7 – Effect of the applied potential on the electrocatalytic current recorded at G/BPhM-CNT electrode, in presence of 0.1 mmol L^{-1} NADH. Experimental conditions: supporting electrolyte, 0.1 mol L^{-1} phosphate buffer (pH 7.0); rotation speed, $n = 500 \text{ min}^{-1}$.

for different NADH concentrations (Fig. 8a), the electrocatalytic rate constant (k_{obs}) was estimated for both G/BPhM and G/BPhM-CNT. Using the dependences of k_{obs}^{-1} vs. [NADH] (Fig. 8b), the $k_{\text{obs},[\text{NADH}]=0}$ were calculated by extrapolating the plots to [NADH] = 0 (Table 2). Thus, the values of $k_{\text{obs},[\text{NADH}]=0}$ in phosphate buffer pH 7 were $51.63 \text{ L mol}^{-1} \text{ s}^{-1}$ for G/BPhM and $856.32 \text{ L mol}^{-1} \text{ s}^{-1}$ for G/BPhM-CNT, and are proving one more the CNTs effect on reaction rate enhancement in NADH oxidation. The $k_{\text{obs},[\text{NADH}]=0}$ value for G/BPhM is smaller than that obtained for graphite electrode modified with another phenothiazine derivative, 16H,18H-dibenzo[c,1]-7,9-dithia-16,18-diazapentacene, ($189 \text{ L mol}^{-1} \text{ s}^{-1}$)³³ but the significant increase of k_{obs} in the presence of CNTs proves that the nanotubes strongly improve the performances of mediators used for NADH oxidation.

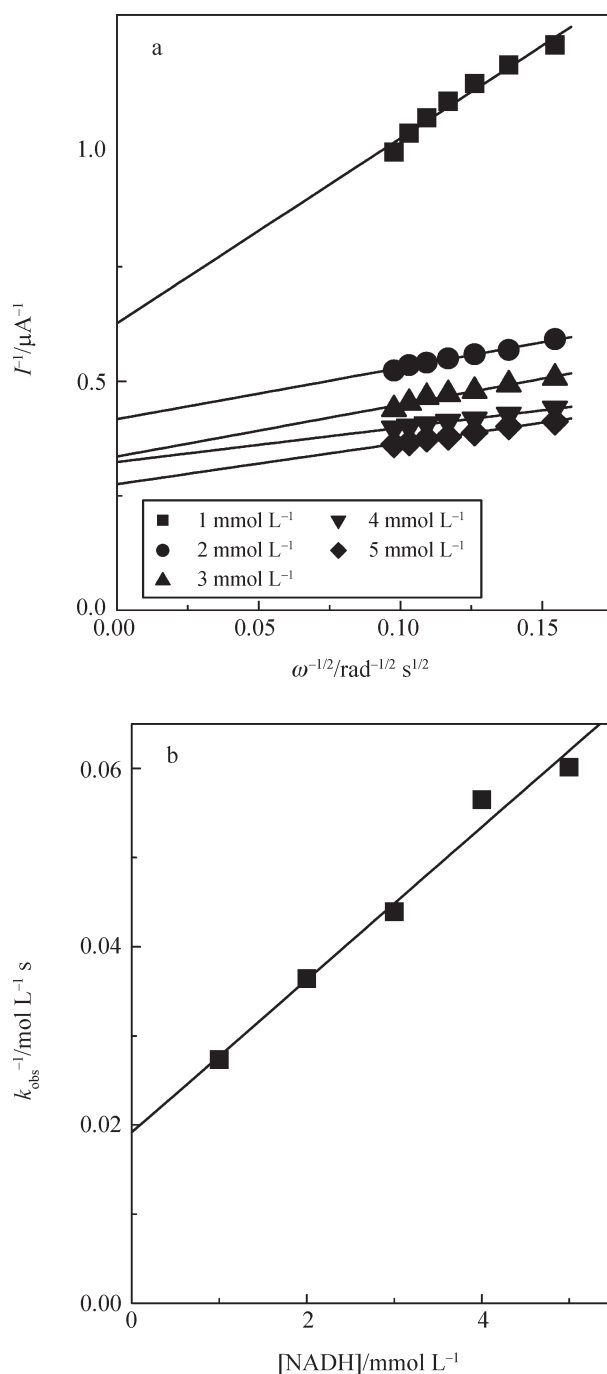


Fig. 8 – Koutecky-Levich plots (a) and variation of k_{obs} with NADH concentration (b) for G/BPhM electrode. Experimental conditions: applied potential, $+100 \text{ mV}$ vs. $\text{Ag}|\text{AgCl}/\text{KCl}_{\text{sat}}$; supporting electrolyte, 0.1 mol L^{-1} phosphate buffer, pH 7.

Table 2 – Electrocatalytic parameters corresponding to the G/BPhM and G/BPhM-CNT modified electrodes. Experimental conditions: applied potential, $+100 \text{ mV}$ vs. $\text{Ag}|\text{AgCl}/\text{KCl}_{\text{sat}}$; supporting electrolyte, 0.1 mol L^{-1} phosphate buffer.

Electrode	pH	$\Gamma/\text{mol cm}^{-2}$	k_{+2}/s^{-1}	$K_M/\text{mmol L}^{-1}$	$k_{\text{obs},[\text{NADH}]=0}/\text{L mol}^{-1} \text{ s}^{-1}$
G/BPhM	7	$3.2 \cdot 10^{-9}$	1.75	33.89	51.63
	6	$1.9 \cdot 10^{-8}$	0.011	0.004	2946.15
G/BPhM-CNT	7	$1.5 \cdot 10^{-8}$	0.074	0.087	856.32
	8	$6.5 \cdot 10^{-8}$	0.027	0.019	145.16

Amperometric sensors for NADH

Amperometric measurements using the rotating disk electrode were carried out in order to study concentration dependences for NADH electrocatalytic process. Successive additions of NADH to the solution were made in order to obtain the dependences of the anodic electrocatalytic current on the NADH concentration. By fitting the amperometric calibration curve to the Michaelis-Menten equation, for G/BPhM and G/BPhM-CNT (Fig. 9), the kinetic and electroanalytical parameters were determined (Table 3). A very fast current response (less than 10 s to reach the steady-state current) after each NADH addition was observed. The electroanalytical parameters are improved by using the CNTs (the sensitivity increases, and the detection limits, calculated considering the signal/noise ratio equal to 3, decrease). These detection limits for NADH are comparable with those presented in literature.^{19,34} It should be mentioned that the performances of NADH sensors

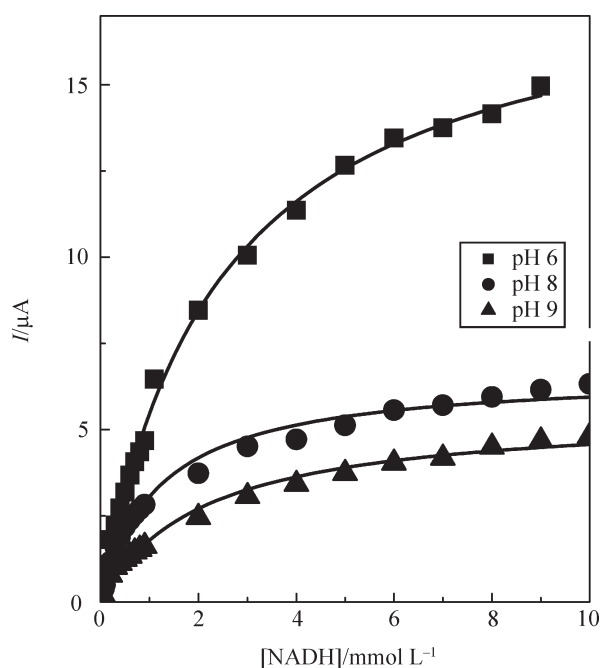


Fig. 9 – Calibration curve for NADH of G/BPhM-CNT electrode. Experimental conditions: applied potential, +100 mV vs. Ag|AgCl/KCl_{sat}; supporting electrolyte, 0.1 mol L⁻¹ phosphate buffer; rotation speed, $n = 500 \text{ min}^{-1}$.

based on G/BPhM-CNT electrodes were obtained at pH 6 and decrease when the pH of supporting electrolyte increases.

Preliminary investigations indicate that the obtained sensor can be used as transducer for amperometric biosensors based on NAD⁺-dehydrogenases, for the detection of some chemical species in real samples (e.g. glucose, ethanol, etc.).

Conclusions

The results detailed above have assessed the ability of coupling CNTs with a new phenothiazine derivative, as a means of improving performances for NADH electrocatalytic oxidation: promoting low potential and high electrocatalytic rate constants $k_{\text{obs},[\text{NADH}] = 0}$. The electrode based on CNTs was found to be stable and can be used as amperometric sensor with improved characteristics for NADH detection.

ACKNOWLEDGEMENTS

Financial support from CNCSIS (Project ID_512) is gratefully acknowledged. The authors thank Dr. Castelia Cristea (Department of Organic Chemistry, “Babes-Bolyai” University Cluj-Napoca, Romania) for providing the phenothiazine derivative.

List of symbols

- E – potential, V
- I – current intensity, μA
- k_s – heterogeneous electron transfer rate constant, s^{-1}
- α – transfer coefficient
- ν – scan rate, V s^{-1}
- Γ – surface concentration, mol cm^{-2}
- $k_{\text{obs}, [\text{NADH}] = 0}$ – electrocatalytic rate constant for NADH oxidation, $\text{L mol}^{-1} \text{s}^{-1}$
- k_{+2} – second order rate constant, s^{-1}
- K_M – Michaelis-Menten constant, mmol L^{-1}
- n – rotation speed, min^{-1}
- R^2 – correlation coefficient
- S – sensitivity, mA L mol^{-1}
- t – time, s
- ω – angular velocity, s^{-1}

Table 3 – Electroanalytical parameters corresponding to obtained modified electrodes. Experimental conditions: as in Fig. 8.

Electrode	pH	detection limit/ $\mu\text{mol L}^{-1}$	linear domain/ mol L^{-1}	$S/\text{mA L mol}^{-1}$	Chi^2	R^2
G/BPhM	7	50	$5 \cdot 10^{-4}$ – 10^{-2}	0.55 ± 0.002	$1.3 \cdot 10^{-14}$	0.996
	6	8	10^{-5} – 10^{-3}	8.3 ± 0.9	$5.6 \cdot 10^{-14}$	0.998
	7	10	10^{-5} – 10^{-3}	6.9 ± 0.6	$36.9 \cdot 10^{-14}$	0.989
G/BPhM-CNT	8	16	$5 \cdot 10^{-5}$ – 10^{-3}	5.6 ± 0.9	$4.1 \cdot 10^{-14}$	0.992
	9	34	$2 \cdot 10^{-5}$ – 10^{-3}	2.6 ± 0.7	$3.0 \cdot 10^{-14}$	0.989

References

1. Valentini, F., Orlanducci, S., Terranova, M. L., Amine, A., Palleschi, G., *Sens. Actuators B* **100** (2004) 117.
2. Rivas, G. A., Rubianes, M. D., Pedano, M. L., Ferreyra, N. F., Luque, G. L., Rodriguez, M. C., Miscoria, S. A., *Electroanalysis* **19** (2007) 823.
3. Guzmán, C., Orozco, G., Verde, Y., Jiménez, S., Godínez, L. A., Juaristi, E., Bustos, E., *Electrochim. Acta* **54** (2009) 1728.
4. Wang, J., Li, M., Shi, Z., Li, N., Gu, Z., *Anal. Chem.* **74** (2002) 1993.
5. Yan, Y., Dong, Z., Shanov, V., Heineman, W. R., Halsall, H. B., Bhattachary, A., Conforti, L., Narayan, R. K., Ball, W. S., Schulza, M. J., *Nanotoday* **2** (2007) 30.
6. Qui, J.-D., Zhou, W.-M., Guo, J., Wang, R., Liang, R.-P., *Anal. Biochem.* **385** (2009) 264.
7. Ye, J.-S., Wen, Y., Zhang, W., Cui, H.-F., Gan, L. M., Xu, G. Q., Sheu, F.-S., *J. Electroanal. Chem.* **562** (2004) 241.
8. Tang, H., Chen, J., Yao, S., Nie, L., Deng, G., Kuang, Y., *Anal. Biochem.* **331** (2004) 89.
9. Qu, S., Wang, J., Kong, J., Yang, P., Chen, G., *Talanta* **71** (2007) 1096.
10. Wang, Y.-R., Hu, P., Liang, Q.-L., Luo, G.-A., Wang, Y.-M., Chin, J., *Anal. Chem.* **36** (2008) 1011.
11. Wang, J., Li, M., Shi, Z., Li, N., Gu, Z., *Electrochim. Acta* **47** (2001) 651.
12. Yogeswaran, U., Chen, S. M., *Electrochim. Acta* **52** (2007) 5985.
13. Gorton, L., *J. Chem. Soc. Faraday Trans. 1* **82** (1986) 1245.
14. Wang, J., *Electroanalysis* **17** (2005) 7.
15. Lawrence, N. S., Wang, J., *Electrochem. Commun.* **8** (2006) 71.
16. Radoi, A., Compagnone, D., Bati, M., Klinar, J., Gorton, L., Palleschi, G., *Anal. Bioanal. Chem.* **387** (2007) 1049.
17. Cristea, C., Cormos, G., Gligor, D., Filip, I., Muresan, L., Popescu, I. C., *J. New Mat. Electr. Sys.* 2009, in press.
18. Murray, R. W., *Electroanalytical Chemistry*, in: Bard, A. J. (Ed.), Vol. 13, Marcel Dekker, New York, 1984.
19. Gligor, D., Dilgin, Y., Popescu, I. C., Gorton, L., *Electrochim. Acta* **54** (2009) 3124.
20. Billon, J. P., *Bull. Soc. Chim. Fr.*, 1960, 1784.
21. Laviron, E., *J. Electroanal. Chem.* **101** (1979) 19.
22. Cauquis, G., Deronzier, A., Lepage, J.-L., Serve, D., *Bull. Soc. Chim. France*, 1977, 295.
23. Lates, V., Gligor, D., Muresan, L., Popescu, I. C., Gropeanu, R., Grosu, I., *Studia Univ. Babeş-Bolyai, Chemia LII* **1** (2007) 11.
24. Arvinte, A., Sesay, A. M., Virtanen, V., Bala, C., *Electroanalysis* **20** (2008) 2355.
25. Agüi, L., Eguílaz, M., Pena-Farfal, C., Yáñez-Sedeno, P., Pingarrón, J. M., *Electroanalysis* **21** (2008) 386.
26. Tu, X., Xie, Q., Huang, Z., Yang, Q., Yao, S., *Electroanalysis* **19** (2007) 1815.
27. Zhu, L., Tian, C., Yang, D., Jiang, X., Yang, R., *Electroanalysis* **20** (2008) 2518.
28. Rubianes, M. D., Rivas, G. A., *Electroanalysis* **17** (2005) 73.
29. Lawrence, N. S., Deo, R. P., Lawrence, N. S., Deo, R. P., Wang, J., *Electroanalysis* **17** (2005) 65.
30. Li, X., Ye, J., *Electroanalysis* **20** (2008) 1917.
31. Zhu, L., Tian, C., Zhu, D., Yang, R., *Electroanalysis* **20** (2008) 1128.
32. Perez-Lopez, B., Sola, J., Alegret, S., Merkoci, A., *Electroanalysis* **20** (2008) 603.
33. Munteanu, F. D., Dicu, D., Popescu, I. C., Gorton, L., *Electroanalysis* **15** (2003) 383.
34. Gligor, D., Dilgin, Y., Popescu, I. C., Gorton, L., *Electroanalysis* **21** (2009) 360.